Highlights

RESEARCH AREA 1 - **Superconductors and Innovative materials for Energy and Environment** - 2022

"Superconductivity induced by structural reorganization in the electron-doped cuprate $Nd_{2-x}Ce_xCuO_4$"

Anita Guarino,[1,2] Carmine Autieri,[3,2] Pasquale Marra,[4,5] Antonio Leo ,[1,2,6] Gaia Grimaldi ,[1,2] Adolfo Avella ,[1,2,7] and Angela Nigro [1,2]
[1]Dipartimento di Fisica "E. R. Caianiello," Università degli Studi di Salerno, 84084 Fisciano (Salerno), Italy
[2]Consiglio Nazionale delle Ricerche CNR-SPIN, UOS Salerno, 84084 Fisciano (Salerno), Italy
[3]International Research Centre Magtop, Institute of Physics, Polish Academy of Sciences, Aleja Lotników 32/46, 02668 Warsaw, Poland
[4]Graduate School of Mathematical Sciences, The University of Tokyo, 3-8-1 Komaba, Meguro, Tokyo, 153-8914, Japan
[5]Department of Physics, and Research and Education Center for Natural Sciences, Keio University, 4-1-1 Hiyoshi, Yokohama, Kanagawa, 223-8521, Japan
[6]NANO_MATES Research Center, Universitá degli Studi di Salerno, 84084 Fisciano (Salerno), Italy
[7]Unitá CNISM di Salerno, Universitá degli Studi di Salerno, 84084 Fisciano (Salerno), Italy

PHYSICAL REVIEW B 105, 014512 (2022)

Electron-doped and hole-doped superconducting cuprates exhibit a symmetric phase diagram as a function of doping. This symmetry is, however, only approximate. Indeed, electron-doped cuprates become superconductors only after a specific annealing process: This annealing affects the oxygen content by only a tiny amount but has a dramatic impact on the electronic properties of the sample. Here we report the occurrence of superconductivity in oxygen-deficient $Nd_{2-x}Ce_xCuO_4$ thin films grown in an oxygen-free environment after annealing in pure argon flow (type A samples). As verified by x-ray diffraction, annealing induces an increase of the interlayer distance between CuO_2 planes in the crystal structure. Since this distance is correlated to the concentration of oxygens in apical positions, and since oxygen content cannot substantially increase during annealing, our experiments indicate that the superconducting phase transition has to be ascribed to a migration of oxygen ions to apical positions during annealing. Moreover, as we confirm via first-principles density functional theory calculations, the changes in the structural and transport properties of the films can be theoretically described by a specific redistribution of the existing oxygen ions at apical positions with respect to CuO_2 planes, which remodulates the electronic band structure and suppresses the antiferromagnetic order, allowing the emergence of hole superconductivity.

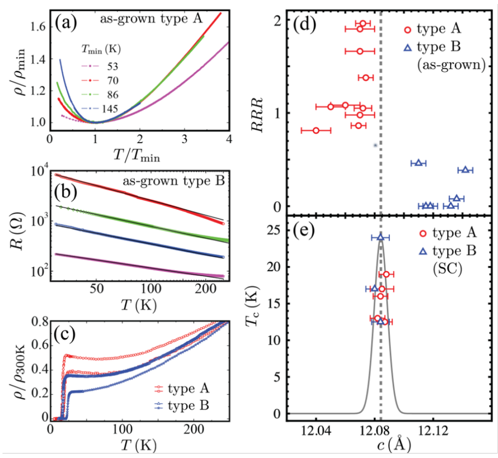

FIG. 2. (a) Resistivity as a function of temperature for type A samples plotted on a log-log scale and normalized to the resistivity minimum. (b) Resistance as a function of temperature for type B samples plotted on a log-log scale. Continuous lines $R(T) \propto T^{-\alpha}$ are the best fit to the data. (c) Normalized resistivity as a function of temperature for type A and B samples after annealing showing the superconducting transition at $T_c \approx 24$K. (d) Residual resistivity ratio *RRR* for as-grown samples (both types) and (e) superconducting critical temperature T_c of samples after annealing as a function of the *c*-axis parameter. The dashed gray line is the average value of c_{SC} and the continuous smooth curve is a guide for the eye. The annealing process was optimized for the sample reaching $T_c \approx 24$K.

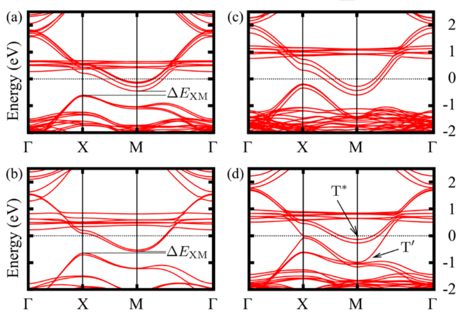

FIG. 3. DFT electronic band structure of NCCO for (a) T* structure with $x = 0.125$, (b) T* structure with $x = 0.25$, (c) T′ structure with $x = 1/6 \approx 0.17$, and (d) $T_{SC} = 2T^* + T'$ structure with $x = 1/6$, where we highlighted the dominant T′ and T* bands with larger contributions. The Fermi level is set to zero. The flat bands at 0.5−1.5 eV above the Fermi level are the cerium 4*f* bands. All other lower-energy bands are copper 3*d* bands.